

THERMAL PERFORMANCE INVESTIGATION OF A MINI NATURAL CIRCULATION LOOP FOR SOLAR PV PANEL OR ELECTRONIC COOLING SIMULATED BY LATTICE BOLTZMANN METHOD

JOHAN AUGUSTO BOCANEGRA, ANNALISA MARCHITTO & MARIO MISALE
DIME – Department of Mechanics, Energetics, Management, and Transportation, Thermal Engineering and Environmental Conditioning Division, University of Genoa.

ABSTRACT

The natural circulation loop (NCL) consists of a thermal-hydraulic system that convoys thermal energy from a heat source to a heat sink without a pump. Applications of those loops can be found in solar energy, geothermal, nuclear reactors, and electronic cooling. The lattice Boltzmann method is a numerical method that can simulate thermal-fluid dynamics, using a mesoscopic approach based on the Boltzmann equation for the density function. A square NCL model with fixed temperatures at the heater and heat sink sections was developed in a bi-dimensional lattice with double distribution dynamics, one distribution for the hydrodynamic field and the other for the thermal field. The different cooler-heater configurations (vertical or horizontal) were investigated. We found that by positioning the source or sink vertically, the flow direction can be controlled. In contrast, in a loop with symmetric horizontal heater - horizontal cooler configuration where both fluid directions are equally probable. The effectiveness of the loop was studied by calculating the heat sink temperature gradient. The lower value was obtained for the horizontal heater horizontal cooler orientation (0.71) and the higher value for the vertical heater vertical cooler configuration with an increment of 34%; simultaneously, the flow rate (Reynolds number) was reduced by 47%.

Keywords: end heat exchanger, heater orientation, heat sink orientation, LBM, thermosyphon.

1 INTRODUCTION

Thermal energy is dissipated from several systems, such as electronics, computers, and mechanical machinery. This dissipated energy can be considered as waste heat. On the other hand, several energy production systems use heat as the primary source, e.g. geothermal generators or nuclear power plants. The heat involved in those systems can be used *efficiently* if optimized technology is used to transport this heat from the source to the desired heat sink. This *efficiency* must consider different thermodynamic factors (as heat transfer effectiveness), environmental factors (as the use of non-toxic substances and reduced energy consumption), and economic factors (as implementation cost and maintenance costs).

Among the systems that need an effective cooling system in a mini-scale (under-meter systems) are common electronics and solar collectors. For example, in electronics and computation, the new trend of mining cryptocurrencies [1, 2] and the use of massive computation clusters and data centers [3] constantly emit heat that must be efficiently transported to a convenient sink (in many applications can be simply the ambient). On the other hand, a very interesting application can be found in the solar energy field: the PV panels work better at low temperatures, then the solar energy can be profited implementing thermal-voltage hybrid systems (PV-T), the heat can be stored and used for water heating [4], or can be used directly for other applications as dryer systems [5].

Natural circulation (or free convection) is of great interest in the energetic and sustainability context because it is possible to convey the thermal energy without using pumps, using closed natural circulation loops (NCLs). Different typologies of NCLs exist. For example, these can be classified by the working fluid typology as single-phase or two-phase NCL. Also, these can be categorized regarding their geometry: the most common geometries are rectangular-shaped or circular-shaped. Some other complex configurations exist as toroidal theta loops [6], parallel-coupled loops [7], or series-coupled loops [8]. The position of the heater and the cooler gives origin to several loop configurations named as horizontal heater horizontal cooler (HHHC), horizontal heater vertical cooler (HHVC), vertical heater horizontal cooler (VHHC), and vertical heater vertical cooler (VHVC) [9]. The use of NCL has, in addition to the mentioned absence of a pump, the great advantage to using different working fluids, like air, water, CO_2 , dielectric fluids, or nanofluids [10, 11], and is common to work with non-toxic materials like water or air as working fluids [12, 13].

This study presents results considering a case study of a (mini) NCL suitable for electronic cooling or solar PV panel cooling. The thermohydraulic performance of the considered systems was simulated by using the lattice Boltzmann method (LBM). This study shows the effects of changing the loop configuration (HHHC, HHVC, VHHC, VHVC) on the flow characteristics and the thermal effectiveness. The HHHC configuration presents a higher flow rate for the same operational conditions.

2 METHODOLOGY

2.1 NCL description

Figure 1 presents a possible application of NCL. This study focus on a single mini-loop with a rectangular shape. The diameter is small, and this selection is not trivial because it is known that stable behavior is achieved if small inner diameters are considered or localized pressure losses are implemented along the circuit [14]. The working fluid is water.

The comparison among the four configurations was made at the same operating conditions in the laminar regime. Those operating conditions can be resumed in the Rayleigh number; in this case, the value 10^6 was selected. A schematic representation of the loop and the tested configurations is presented in Fig. 2. The loop considered here works with the fixed temperature at the heater (T_H) and cooler (T_C), also known as *NCL with heat end exchangers* [15]. Recently was shown that this kind of square mini-loops can work connected in parallel to convey more thermal energy, and the thermohydraulic performance remains stable even if the heating power in one circuit changes [7, 16].

2.2 LBM for thermal flow

The LBM is a numerical method used to simulate fluids by solving the discretized Boltzmann equation (LBE) eqn (1). This relationship expresses the balance between transport and collision processes when a statistical approach over the molecules of the fluid is considered. Complex boundaries and vorticity can be simulated by this numerical method [17]. A review of the application of this method in nuclear reactor problems, including thermal flows and neutronics, can be found in Bocanegra *et al.* [18].

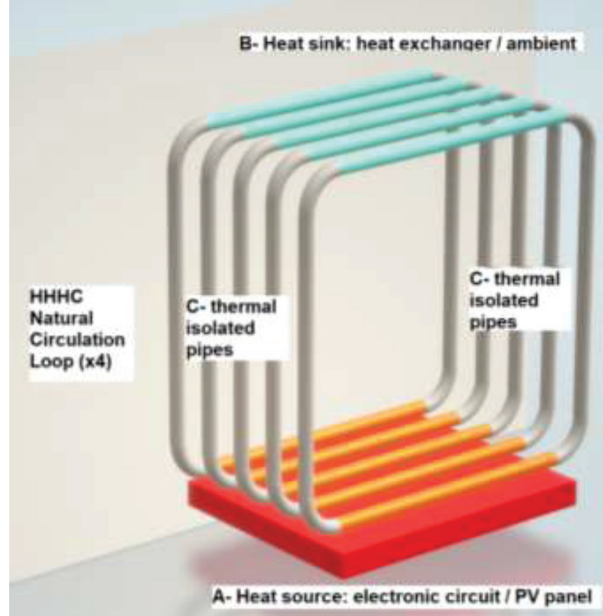


Figure 1: Application example: four NCLs in HHHC configuration transport the heat from A (circuit or PV panel, hot temperature) to B (heat sink, cold temperature). The number of loops can vary for each application.

$$f_i(\mathbf{r} + \mathbf{c}_i \Delta t, t + \Delta t) - f_i(\mathbf{r}, t) = -\frac{1}{\tau} (f_i(\mathbf{r}, t) - f_i^{eq}(\mathbf{r}, t)) + \Delta t F_i \quad (1)$$

The evolution of the probability density function f_i is described by the LBE. The probability density function f_i represents the probability of finding a molecule with a given velocity in each position \mathbf{r} and time t . This probabilistic approach is possible considering a discretization of space $\Delta \mathbf{r}$, time Δt , and velocity \mathbf{c}_i . In this way, a lattice structure propagates the density function in given directions characterized by the discretized velocity set \mathbf{c}_i . The lattice structure used for the simulation is known as D2Q9. To simulate the temperature field and additional distribution function, g_i was used with a D2Q5 lattice structure, eqn (2). The double distribution function approach has been applied successfully to diverse thermal fluid dynamics problems, e.g. natural circulation in cavities or heat transfer in a microchannel [19]. The two-way coupling between the hydraulic field and the thermal field was achieved by considering a forcing term F_i proportional to the local temperature representing the buoyancy force (Boussinesq hypothesis). The approach adopted is similar to the one presented by Guo *et al.* [20]

$$g_i(\mathbf{r} + \mathbf{c}_i \Delta t, t + \Delta t) - g_i(\mathbf{r}, t) = -\frac{1}{\tau_g} (g_i(\mathbf{r}, t) - g_i^{eq}(\mathbf{r}, t)) \quad (2)$$

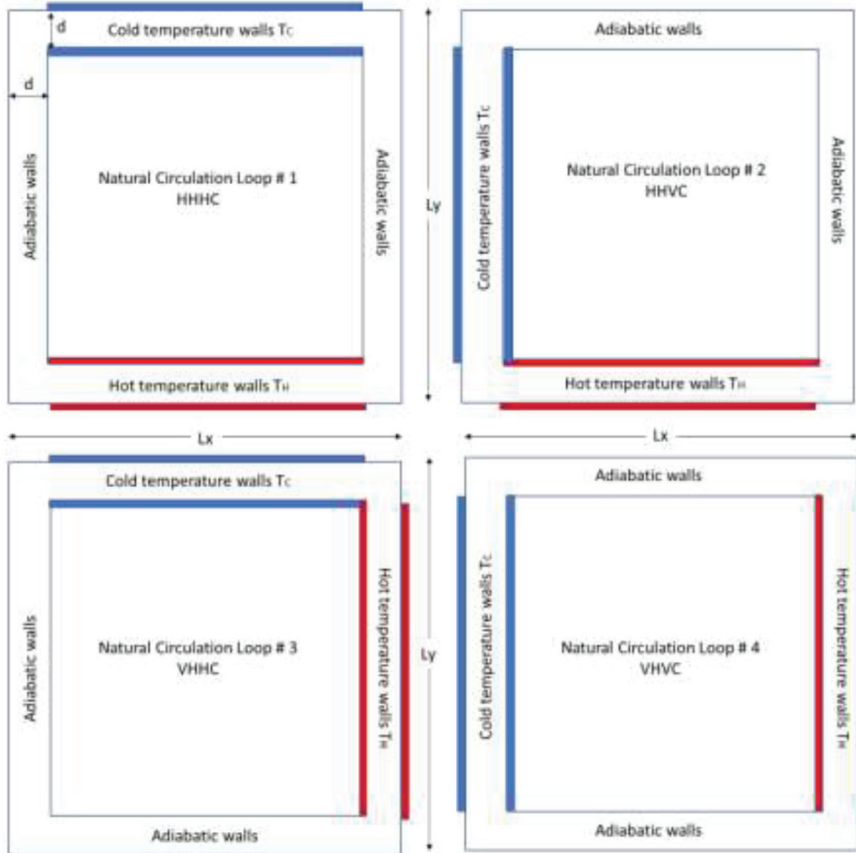


Figure 2: Loop configurations: horizontal heater horizontal cooler (HHHC), horizontal heater vertical cooler (HHVC), vertical heater horizontal cooler (VHHC), and vertical heater vertical cooler (VHVC). $L_x = L_y = 0.250$ m, pipe diameter $d = 0.010$ m.

The equilibrium distributions f_i^{eq} and g_i^{eq} are calculated as a Taylor expansion of the Maxwell–Boltzmann distribution using the velocity and truncated holding second-order terms. τ, τ_g represent a time scale for the relaxation to equilibrium process the kernel of the collision algorithm presented on the right-hand side of eqns (1) and (2). τ is proportional to the viscosity γ . The ratio of these two relaxation times is equivalent to the Prandtl number (Pr) of the simulated fluid; in our case, we use $Pr=7.0$. More details of the LBM can be found in [21–23].

Some advantages of the LBM are linked to the parallelization capabilities by the application of local collision and streaming rules in each iteration, and the easy handle of complex geometry using the lattice structure instead of the typical meshing algorithms used in common CFD methods.

The code used for the simulations was implemented in C++ using the PALABOS library [24]. Message passing interface (MPI) standard library was used for the parallel implementation and run of the code on an Intel® Xeon® Platinum 8260 CPU, 2.40 GHz, workstation using 46 cores. The average velocity for the runs is 157 Mega site updates per second (MSUPS).

3 RESULTS AND DISCUSSION

3.1 Model validation

The numerical model was validated by contrast with the analytical and empirical model proposed by Cheng *et al.* [25] for a single-phase NCL in HCHH configuration with fixed temperature boundaries. All the expressions used for validation were previously verified experimentally by Cheng *et al.* [25]. The numerical results were compared with the physical values using non-dimensional groups and normalized variables. The temperature was normalized using 0 for the heat sink and 1 for the heater. The velocity was normalized using the maximum steady-state velocity along the loop. The steady-state Reynolds number ($Re_{ss} = v_{rms}^{ss} d / \gamma$) is referenced to the pipe diameter d and is proportional to the rms velocity (and flow rate), e.g. a rms velocity of 0.001 m/s is equivalent to a $Re_{ss}=10$, approximately. Accordance between the analytical model and the LBM results for the thermal field was observed, details are provided in Fig. 7a. In the same manner were contrasted the analytical equation to determine the steady-state Reynolds number (error below 5%) and the empirical relationship for the Nusselt number (error below 15%). Additionally, the performance of the boundary conditions was evaluated by contrasting the parabolic velocity cross-section profile into the pipes with a very good fitting and confirm the no-slip boundary condition imposed. The thermal boundary conditions were verified by observing the temperature gradient near the adiabatic walls, and near-zero values were found. After that validation, the model was modified to study the effect of locating the cooler and heater in vertical positions. The detailed contrast with the analytical model under different operation conditions is object of a future work.

3.2 Fluid velocity profile

As was expected, the HHHC loop is the only symmetrical configuration considered, and the flow in both senses (clockwise and counterclockwise) is possible. We observe this fact under several runs of the code. On the other hand, the vertical position of the cooler or the heater forces the flow in the loop in the considered geometry in a counterclockwise sense. Figure 3 shows the flow under the four configurations analyzed here.

In Fig. 3, the flow pattern is laminar in all the cases. The velocity decreases to zero near the walls and presents the maximum in the center of the tube. However, some small perturbances are noted at the corners, probably by the 90° elbows. Moreover, a big deviation for the expected parabolic profile was noted at the inlet of the vertical heaters or coolers. This effect can be explained by the buoyancy force acting against the fluid flow in those vertical pipes. This interesting fact is depicted in Fig. 4a; the cross-section velocity profile at different locations along the vertical heater shows a sensible decrease of the velocity at the center near the inlet (three diameters), and then the effect vanishes, and the parabolic profile is developed. Figure 4b depicts the longitudinal velocity profile for the VHVC loop to illustrate this phenomenon at the center of the pipe. However, the effect on the cross-section averaged velocity is almost imperceptible.

Figure 5 shows the transient behavior of the four circuits. The oscillation during the transient is more evident for the HHHC configuration, similar for HHVC and VHHC, and very reduced for VHVC. Also, it is visible in the figure that the time to arrive at the steady state changes for each configuration. Similar behaviors were experimentally observed by Vijayan

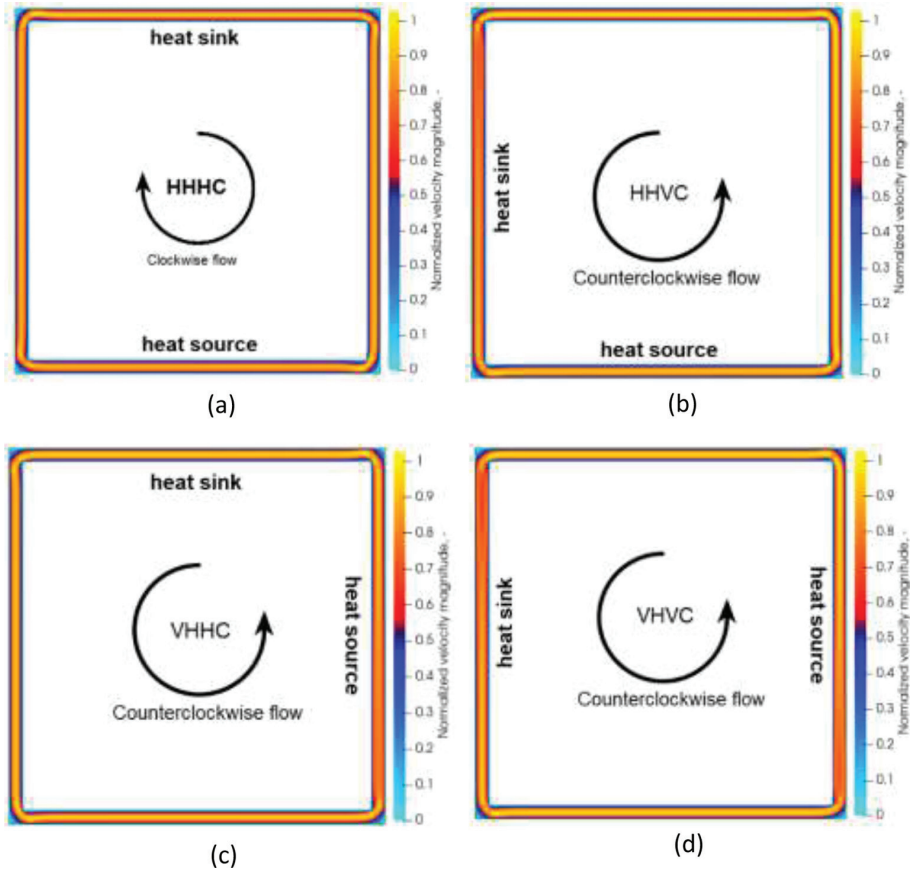


Figure 3: Normalized velocity magnitude and flow direction along the loops at steady-state
 (a) HHHC; (b) HHVC; (c) VHHC; (d) VHVC.

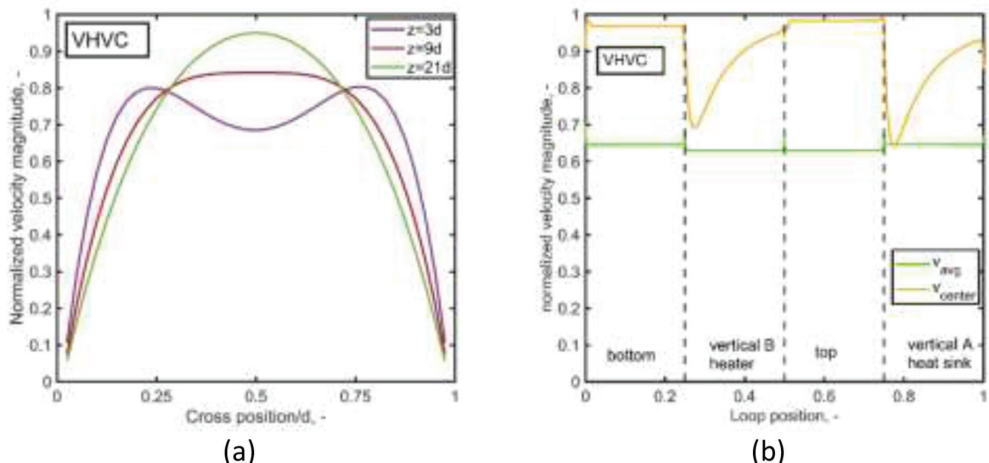


Figure 4: VHVC velocity profile: (a) Cross-section and (b) longitudinal section at the center of the pipe v_{center} and cross-section average velocity v_{avg} .

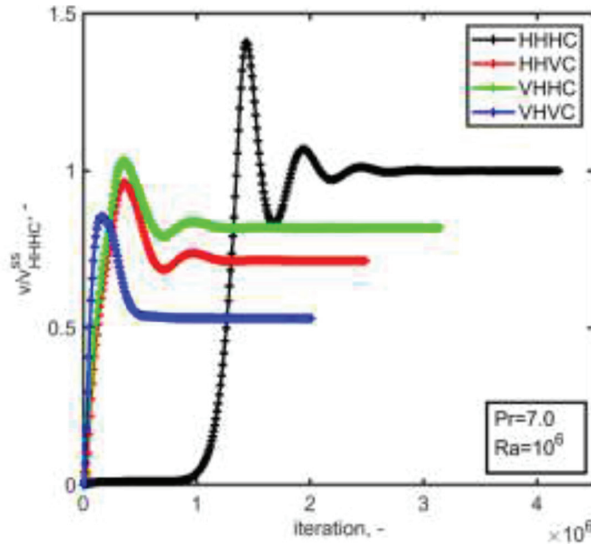


Figure 5: Transient of the velocity, normalized to the HHHC velocity at steady state.

et al. [26] and Chen *et al.* [27]. They found experimentally that for HHHC and HHVC, the time to start the circulation is higher than the time to start the flow with vertical heaters, in which cases the flows start when the heating power is provided.

3.3 The thermal field at steady state

Figure 6 shows the thermal field at the steady state. It is notorious that the main temperature gradient is obtained at the heaters and heat sinks. Moreover, the other pipes present a minimum temperature variation. In fact, this figure provides a visual probe of the adiabatic condition of those unheated pipes. Also, it is interesting to note that in the HHHC, one adiabatic pipe is hot, and the other is cold, as in the VHVC configuration. On the other hand, the HHVC and VHHC configurations have only one adiabatic section, hot and cold, respectively. Figure 7 presents the normalized temperature profile along the longitudinal axe.

3.4 Thermohydraulic performance

To compare the performance of the four circuits, some parameters and non-dimensional groups were calculated (Table 1). The percentual differences referenced to the HHHC values are included for the HHVC, VHHC, and VHVC loops.

Table 1 shows the simulation steps needed to reach the steady state. The Reynolds number referenced to the pipe diameter is used to evaluate the flow regime. It is noted that the highest value is obtained in the HHHC configuration. The Nusselt number expresses the proportion between the convective and conductive heat transfer. The average Nusselt number was numerically calculated for the heater in all the configurations using the temperature gradient near the wall. The theoretical Nusselt number for the HHHC configuration was calculated by fitting the thermal profile to the Cheng *et al.* model ($Nu = 1.60$) and using the empirical correlation proposed by them ($Nu = 1.43$). This value is lower than the common value for straight

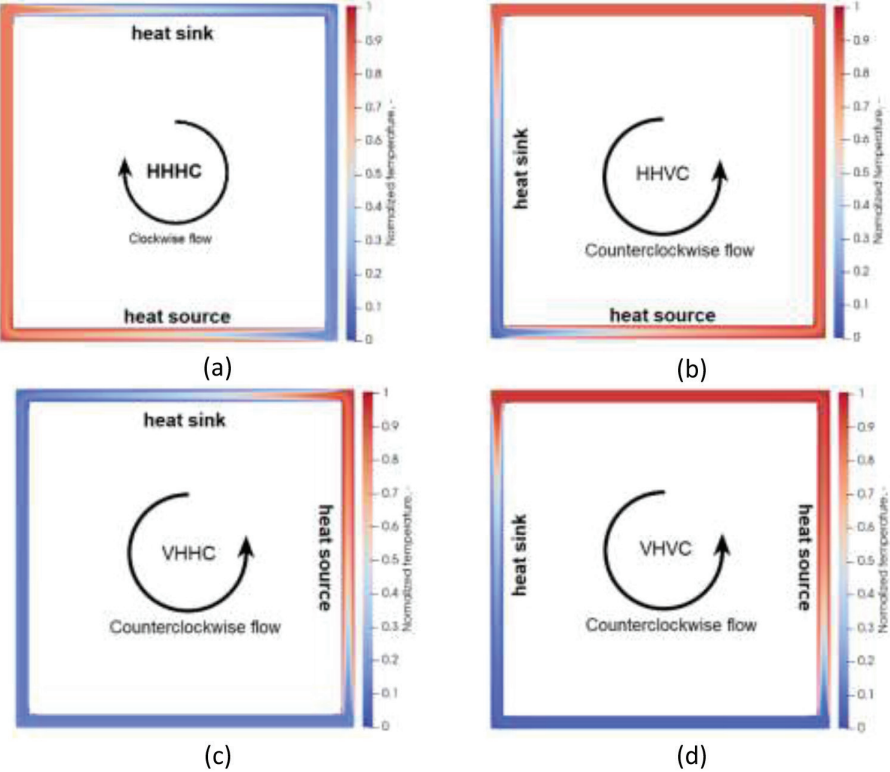


Figure 6: Thermal field and flow direction along the loops at steady state. (a) HHHC, (b) HHVC, (c) VHHC, (d) VHVC.

pipes $Nu = 3.66$. The highest value was observed for the HHHC configuration. The temperature difference at the heat sink inlet and outlet is included $T_{sink}^{in} - T_{sink}^{out}$, the highest value was obtained for the VHVC configuration. Using the temperature values at the inlet T_{sink}^{in} and T_{sink}^{out} outlet of the heat sink, it is possible to obtain the effectiveness, eqn (3), by comparing the steady-state temperature difference $T_{sink}^{in} - T_{sink}^{out}$, with the maximum possible difference $T_{sink}^{in} - T_C$. The highest heat sink effectiveness was found in the VHVC configuration.

$$\varepsilon_{sink} = \frac{T_{sink}^{in} - T_{sink}^{out}}{T_{sink}^{in} - T_C} \quad (3)$$

4 CONCLUSIONS

A bi-dimensional model of a single-phase NCL with heat end exchangers was simulated using the LBM with double distribution functions. The model was validated using the model proposed by Cheng *et al.* [25] equivalent to Vijayan's laminar regime model [12] for the Horizontal Heater Horizontal Cooler configuration. The effect of considering different configurations for the loop was presented for the transient and the steady state. Moreover, the observations agree with previous observations presented by Vijayan *et al.* [26].

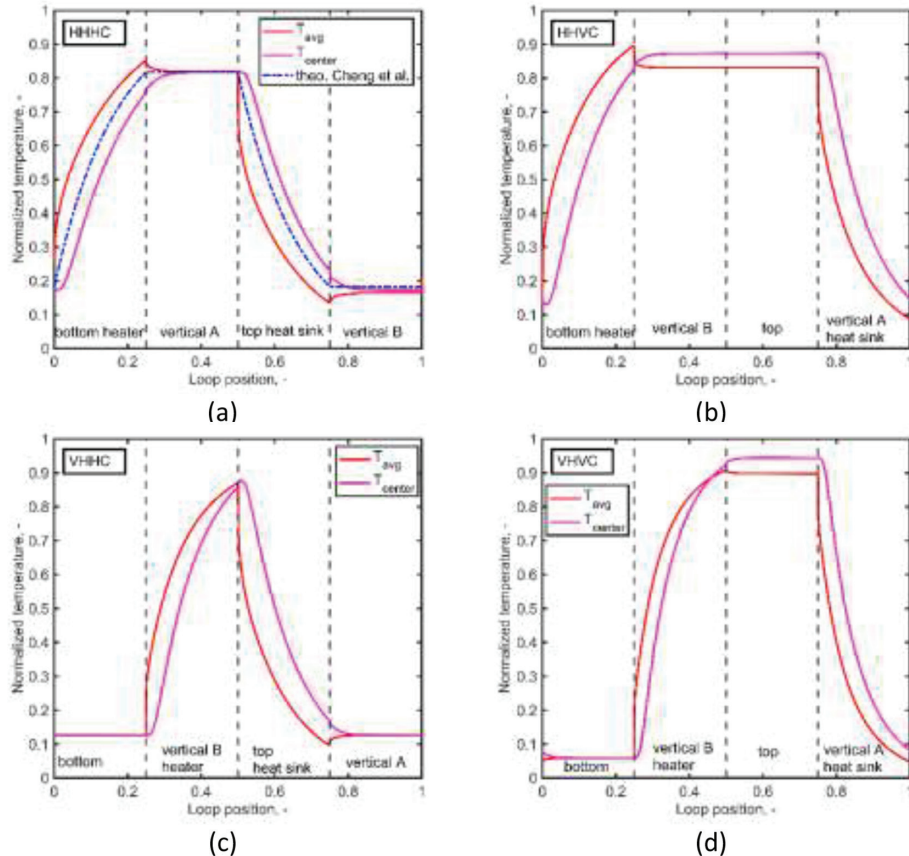


Figure 7: Temperature profile at steady state along the loop (following the flow direction). (a) HHHC, (b) HHVC, (c) VHHC, (d) VHVC.

- The HHHC configuration gives the highest flow rate.
- Disturbances in the parabolic velocity profile were observed at the inlet of the vertical section that contains the heater or cooler.
- The natural circulation takes more time to take place in the HHHC configuration, and this time is similar for the other three configurations.
- The time to reach the steady state going from low to high is VHVC, HHVC, VHHC, and HHHC, respectively.
- The VHVC configuration reached higher heat sink effectiveness.
- The highest Nusselt number was obtained in the HHHC configuration.

Finally, this study shows that this kind of square loop is suitable for cooling systems of small components (as electronics or solar PV panels) in all the studied configurations. Under the tested operational parameters, all the loops remain in the laminar regime; the dynamic was stable (no flux inversion), and all reached a steady state. However, the thermohydraulic performance depends strongly on the selected configuration. The two extreme cases were the

Table 1: Thermohydraulic parameters were evaluated at steady state, considering the four heater-cooler configurations. The comparison took the HHHC values as a reference.

Non-dimensional parameter	Loop configuration			
	HHHC	HHVC	VHHC	VHVC
Transient time, timesteps	4,195,300	2,494,300	3,143,900	2,013,000
		-41%	-25%	-52%
Reynolds number:	15.2	10.9	12.5	8.1
		-28%	-18%	-47%
Heater Nusselt number:	1.78	0.43	0.43	0.37
		-76%	-76%	-79%
Heat sink temperature difference:	0.58	0.74	0.70	0.85
		+28%	+21%	+47%
Heat sink effectiveness:	0.71	0.89	0.80	0.94
		+25%	+13%	+32%

HHHC (with the highest Reynolds number at steady state and lower sink effectiveness) and the VHVC (with the lowest Reynolds number at steady state and higher sink effectiveness). On the other hand, the performance of the HHVC and VHHC is similar. Future research must be done concerning the variation of the thermohydraulic performance at different temperature gaps, i.e. varying the Rayleigh number.

ACKNOWLEDGMENT

This research was funded by Ministero dell’Istruzione, dell’Università e della Ricerca (MIUR, Italy), grant number PRIN-2017F7KZWS.

REFERENCES

- [1] Náñez Alonso, S.L., Jorge-Vázquez, J., Echarte Fernández, M.Á. & Reier Forradellas, R.F., Cryptocurrency mining from an economic and environmental perspective. *Energies*, **14**, pp. 4254, 2021. <https://doi.org/10.3390/en14144254>
- [2] de Vries, A., Bitcoin’s growing energy problem. *Joule*, **2**, pp. 801–805, 2018. <https://doi.org/10.1016/j.joule.2018.04.016>
- [3] Huang, P., Copertaro, B., Zhang, X., Shen, J., Löfgren, I., Rönnelid, M., Fahlen, J., Andersson, D. & Svanfeldt, M., A review of data centers as prosumers in district energy systems: renewable energy integration and waste heat reuse for district heating. *Applied Energy*, **258**, pp. 114109, 2020. <https://doi.org/10.1016/j.apenergy.2019.114109>
- [4] Ju, X., Xu, C., Liao, Z., Du, X., Wei, G., Wang, Z. & Yang, Y., A review of concentrated photovoltaic-thermal (CPVT) hybrid solar systems with waste heat recovery (WHR). *Science Bulletin*, **62**, pp. 1388–1426, 2017. <https://doi.org/10.1016/j.scib.2017.10.002>

- [5] Al-Kaiyiem, H.H., Hybrid techniques to enhance solar thermal: the way forward. *Int. J. EQ.*, **1**, pp. 50–60, 2015. <https://doi.org/10.2495/EQ-V1-N1-50-60>
- [6] Satou, A. Madarame, H. & Okamoto, K., Unstable behavior of single-phase natural circulation under closed loop with connecting tube. *Experimental Thermal and Fluid Science*, **7**, 2001.
- [7] Misale, M., Bocanegra, J.A., Borelli, D. & Marchitto, A., Experimental analysis of four parallel single-phase natural circulation loops with small inner diameter. *Applied Thermal Engineering*, **180**, pp. 115739, 2020. <https://doi.org/10.1016/j.applthermaleng.2020.115739>
- [8] Dass, A. & Gedupudi, S., Numerical investigation on the heat transfer coefficient jump in tilted single-phase natural circulation loop and coupled natural circulation loop. *International Communications in Heat and Mass Transfer*, **120**, pp. 104920, 2021. <https://doi.org/10.1016/j.icheatmasstransfer.2020.104920>
- [9] Misale, M., Overview on single-phase natural circulation loops, in: International Conference on Advances in: Mechanical & Automation Engineering, Rome, Italy, 2014: p. 13.
- [10] Misale, M., Devia, F. & Garibaldi, P., Experiments with Al₂O₃ nanofluid in a single-phase natural circulation mini-loop: Preliminary results. *Applied Thermal Engineering*, **40**, pp. 64–70, 2012. <https://doi.org/10.1016/j.applthermaleng.2012.01.053>
- [11] Garibaldi, P. & Misale, M., Experiments in single-phase natural circulation miniloops with different working fluids and geometries. *J. Heat Transfer*, **130**, pp. 104506, 2008. <https://doi.org/10.1115/1.2948393>
- [12] Vijayan, P.K., Experimental observations on the general trends of the steady state and stability behaviour of single-phase natural circulation loops. *Nuclear Engineering and Design*, **215**, pp. 139–152, 2002. [https://doi.org/10.1016/S0029-5493\(02\)00047-X](https://doi.org/10.1016/S0029-5493(02)00047-X)
- [13] Misale, M., Experimental study on the influence of power steps on the thermohydraulic behavior of a natural circulation loop. *International Journal of Heat and Mass Transfer*, **99**, pp. 782–791, 2016. <https://doi.org/10.1016/j.ijheatmasstransfer.2016.04.036>
- [14] Misale, M. & Frogheri, M., Influence of pressure drops on the behavior of a single-phase natural circulation loop: preliminary results. *International Communications in Heat and Mass Transfer*, **26**, pp. 597–606, 1999. [https://doi.org/10.1016/S0735-1933\(99\)00046-9](https://doi.org/10.1016/S0735-1933(99)00046-9)
- [15] Cheng, H., Lei, H. & Dai, C., Thermo-hydraulic characteristics and second-law analysis of a single-phase natural circulation loop with end heat exchangers. *International Journal of Thermal Sciences*, **129**, pp. 375–384, 2018. <https://doi.org/10.1016/j.ijthermalsci.2018.03.026>
- [16] Misale, M., Bocanegra, J.A. & Marchitto, A., Thermo-hydraulic performance of connected single-phase natural circulation loops characterized by two different inner diameters. *International Communications in Heat and Mass Transfer*, **125**, p. 105309, 2021. <https://doi.org/10.1016/j.icheatmasstransfer.2021.105309>
- [17] Arumuga Perumal, D. & Dass, A.K., Simulation of flow in two-sided lid-driven square cavities by the lattice Boltzmann method, in: The New Forest, UK, 2008: pp. 45–54. <https://doi.org/10.2495/AFM080051>
- [18] Bocanegra Cifuentes, J.A., Borelli, D., Cammi, A., Lomonaco, G. & Misale, M., Lattice Boltzmann method applied to nuclear reactors—a systematic literature review. *Sustainability*, **12**, p. 7835, 2020. <https://doi.org/10.3390/su12187835>

- [19] Sousa, A.C.M., Hadavand, M. & Nabovati, A., Three-dimensional simulation of slip-flow and heat transfer in a microchannel using the lattice Boltzmann method, in: Tallinn, Estonia, pp. 75–85, 2010. <https://doi.org/10.2495/HT100071>
- [20] Guo, Z., Shi, B. & Zheng, C., A coupled lattice BGK model for the Boussinesq equations. *Int. J. Numer. Meth. Fluids*, **39**, pp. 325–342, 2002. <https://doi.org/10.1002/fld.337>
- [21] Succi, S., The Lattice Boltzmann *Equation for Fluid Dynamics and Beyond*, Clarendon Press, Oxford, England, 2001.
- [22] Succi, S., Benzi, R. & Massaioli, F., A review of the Lattice Boltzmann method. *International Journal of Modern Physics C*, **4**, pp. 409–415, 1993.
- [23] Arumuga Perumal, D. & Dass, A.K., A review on the development of lattice Boltzmann computation of macro fluid flows and heat transfer. *Alexandria Engineering Journal*, **54**, pp. 955–971, 2015. <https://doi.org/10.1016/j.aej.2015.07.015>
- [24] Latt, J., Malaspinas, O., Kontaxakis, D., Parmigiani, A., Lagrava, D., Brogi, F., Belgacem, M.B., Thorimbert, Y., Leclaire, S., Li, S., Marson, F., Lemus, J., Kotsalos, C., Condradín, R., Coreixas, C., Petkantchin, R., Raynaud, F., Beny, J. & Chopard, B., Palabos: Parallel Lattice Boltzmann Solver. *Computers & Mathematics with Applications*, p. S0898122120301267, 2020. <https://doi.org/10.1016/j.camwa.2020.03.022>
- [25] Cheng, H., Lei, H., Zeng, L. & Dai, C., Theoretical and experimental studies of heat transfer characteristics of a single-phase natural circulation mini-loop with end heat exchangers. *International Journal of Heat and Mass Transfer*, **128**, pp. 208–216, 2019. <https://doi.org/10.1016/j.ijheatmasstransfer.2018.08.136>
- [26] Vijayan, P.K., Sharma, M. & Saha, D., Steady state and stability characteristics of single-phase natural circulation in a rectangular loop with different heater and cooler orientations. *Experimental Thermal and Fluid Science*, **31**, pp. 925–945, 2007. <https://doi.org/10.1016/j.expthermflusci.2006.10.003>
- [27] Chen, L., Zhang, X.-R. & Jiang, B., Effects of heater orientations on the natural circulation and heat transfer in a supercritical CO₂ rectangular loop. *Journal of Heat Transfer*, **136**, p. 052501, 2014. <https://doi.org/10.1115/1.4025543>